# A Very High-Order (VHO) Flux Reconstruction (FR) Formulation for the Numerical Simulation of the 1D Two-Fluid Four-Equation Model in Pipelines

Anderson V. do Nascimento[1], Cleuber E. N. Silva[2], Giselle M. L. L. da Silva[3], Tiago C. Freitas[4], Rosane A. Fontes[5], Mônica T. da Silva[6], Jussara de M. Silva[7], Paulo R. M. Lyra[8], Alessandro R. E. Antunes[9], Darlan K. E. de Carvalho[10]

[1]*Programa de Pós-Graduação em Engenharia Civil (PPGEC), CTG – UFPE, Av. Acadêmico Hélio Ramos, s/n, CEP, Recife, PE 50740-530 Brazil, anderson.viananascimento@ufpe.br*
[2]*Programa de Pós-Graduação em Engenharia Civil (PPGEC), CTG – UFPE, Av. Acadêmico Hélio Ramos, s/n, CEP, Recife, PE 50740-530 Brazil, cleuber.silva@ufpe.br*
[3,4,5,6,7]*Petróleo Brasileiro S.A. (PETROBRAS) - Petróleo Brasileiro - Rio de Janeiro - Matriz, Petróleo Brasileiro – Rio de Janeiro. Avenida Melício Machado, s/n km 1 - Atalaia 49037445 - Aracaju, SE, Brasil, gisellelopes@petrobras.com.br, ticfreitas@petrobras.com.br, rafontes@petrobras.com.br, monicats@petrobras.com.br, jussarams@petrobras.com.br*
[8,10]*Departamento de Engenharia Mecânica, CTG – UFPE, Av. Acadêmico Hélio Ramos, s/n, CEP, Recife, PE 50740-530 Brazil, paulo.lyra@ufpe.br*
[9]*Núcleo de Tecnologia, CAA – UFPE, Rod. BR-104 – Km 59 – Nova Caruaru CEP, Caruaru, PE 55002-970, Brazil, alessandro.antunes@ufpe.br*

**Abstract.** The numerical modeling of multiphase and multicomponent fluid flow in pipelines is essential for addressing various industrial challenges. In the oil industry, accurate knowledge of key flow parameters, such as velocities, pressures, and void fractions, is crucial for managing flow assurance issues. However, simulating flow inside oil pipelines remains a challenging task, as these ducts can extend for thousands of meters. Therefore, mathematical model simplifications are necessary to make the computational cost of CFD simulations feasible. The primary simplification is treating the flow as one-dimensional (1D), as implemented in commercial software such as ALFAsim, LedaFlow, and OLGA. However, these software packages still rely on first-order schemes to handle the advective terms of their governing equations. Among the available mathematical models for simulating 1D two-phase flow in pipelines, the two-fluid model is one of the main alternatives and can even be formulated as a particular case of the more general multi-field model commonly used in commercial packages. The main objective of this study is to develop and implement a very high-order (VHO) scheme in the two-fluid four-equation model, specifically using the Flux Reconstruction (FR) method. The FR method is implemented with a hierarchical limiting scheme for p-type adaptation, and two different correction functions are used and evaluated, leading to two variations of the method that transition from Nodal Discontinuous Galerkin (NDG) to Spectral Difference (SD) methods. The pressure correction equation is derived from mass conservation, and a semi-implicit pressure-based SIMPLE-like method is used for coupling. The pressure equation is solved using the Two-Point Flux Approximation (TPFA) finite volume technique with a staggered grid arrangement. Different test cases are analyzed to evaluate the performance of the FR method. The results demonstrate promising accuracy and are consistent with those reported in the literature, highlighting the potential of the FR method for advancing flow simulations in pipelines.

**Keywords:** 1-D Fluid Flow in Pipelines, Four-Equation Single-Pressure Two-Fluid Model, Very High-Order (VHO) Approximation, Flux Reconstruction (FR).

# 1 Introduction

In various engineering fields, simulating multiphase flow in pipelines is crucial for process management. Knowledge of multiphase flow parameters, such as phase velocities, volumetric fractions of each phase, pressures, density, among others, is essential for managing the continuity of the flow in pipelines [1]. In the oil industry, for instance, predicting these parameters is of utmost importance for managing flow assurance within riser pipelines.

Flow assurance deals with challenges such as the formation and accumulation of scales, hydrates, and waxes, in addition to issues like pipeline corrosion and erosion. These phenomena must be properly addressed to avoid both safety risks and economic losses [1]. Predicting such problems becomes particularly complex in long-distance pipelines, such as oil risers that can span several kilometers. In this context, CFD (Computational Fluid Dynamics) simulations represent the most practical approach for anticipating these issues. Nonetheless, due to computational constraints, it is necessary to apply substantial simplifications. One of the main simplifications is to consider the flow as spatially one-dimensional (1-D), a strategy widely adopted by commercial simulators developed for analyzing oil risers—examples include ALFAsim, LedaFlow, and OLGA [2], [3], [4].

In simulations involving two-phase flows, one of the most representative one-dimensional mathematical formulations is the two-fluid 1D model [5], which captures the distinct dynamics of each phase. This framework is built upon a set of coupled non-linear partial differential equations that individually express the conservation of mass, momentum, and energy for each phase [6]. Over the years, multiple formulations have emerged for this class of models, differing in their mathematical derivation and numerical implementation strategies [6], [7].

A widely referenced version in scientific literature is the four-equation single-pressure model, where both phases are assumed to share a common pressure field. This formulation is often viewed as the isothermal simplification of the more comprehensive six-equation version of the two-fluid single-pressure model [5], [8]. Such models are implemented in several reactor thermal-hydraulics codes, including RALAP, TRAC, and CATHARE [9], [10]. Despite their relative simplicity in terms of implementation, single-pressure approaches are known to be susceptible to Kelvin–Helmholtz-type instabilities, particularly when two fluids interact under a shared pressure field [11]. These instabilities are primarily linked to the system losing hyperbolicity [12], [13]. A well-established method for mitigating this issue is the application of the CATHARE model [12], which introduces an interfacial pressure difference to recover hyperbolicity in the governing equations [13].

From a numerical standpoint, staggered mesh techniques combined with donor-cell differencing are frequently employed to enhance stability in single-pressure two-fluid simulations [8], [14]. However, these lower-order methods often induce numerical diffusion, which can deteriorate the fidelity of the results. To improve accuracy, higher-order discretization schemes are typically adopted. Among the most prominent are: the MUSCL (Monotonic Upstream-centered Scheme for Conservation Laws) introduced by van Leer [15]; the Spectral Volume (SV) method, extensively explored by Wang and Liu [16], [17], [18], [19], [20]; the Spectral Difference (SD) method developed by Liu and collaborators [21]; and the Flux Reconstruction (FR) approach by Huynh [22]. This last method has recently been extended by members of this research team to handle complex multiphase and multicomponent flow phenomena in porous media [23-28].

In the present work, we implement the very high-order flux-reconstruction (FR) method to improve the accuracy and efficiency of the two-fluid model. In our context, the flux-reconstruction method was used to solve the mass conservation and the momentum conservation equations of the two-fluid four-equation single-pressure model. To validate the accuracy of our formulation, we present and discuss the numerical results for some benchmark problems [13], [29].

# 2 Mathematical formulation

The two-fluid model is characterized by solving the governing conservation equations separately for each phase. The two-fluid four-equation model is composed by two continuity equations and two momentum equations, that were adapted for the 1-D, compressible, inviscid and isothermal flow. The continuity equation, for phase $k$ = $L$ $(liquid)$, $G$ $(gas)$, can be written as:

$$\frac{\partial}{\partial t}(\alpha_k \rho_k) + \frac{\partial}{\partial x}(\alpha_k \rho_k u_k) = 0 \tag{1}$$

where $\alpha_k$ represents the volumetric fraction occupied by phase $k$ in the section, $\rho_k$ represents the density and $u_k$

the velocity. Using the same terms, we can write the momentum equation, for phase $k$, as:

$$\frac{\partial}{\partial t}(\alpha_k \rho_k u_k) + \frac{\partial}{\partial x}(\alpha_k \rho_k u_k^2) = -\alpha_k \frac{\partial p_k}{\partial x} - (p_k - p_k^i)\frac{\partial \alpha_k}{\partial x} + \alpha_k \rho_k g \sin\theta \tag{2}$$

where $p$ is the pressure shared by the phases, $g$ is the acceleration of gravity, θ is the pipe slope, and $p_k^i$ is the interface pressure in phase $k$. In this momentum equation, the influence of mass transfer, wall friction, and interface friction are ignored.

## 3 Numerical Formulation

In the present work, we use the FR method [22] to solve the advective terms of the continuity and moment equations. Using the FR method, first the advected variables ($u_k$ and $\alpha_k$) are interpolated and recovered in a discontinuous strategy. The degree of the interpolating polynomial defines the approximation order of the method and the points location for interpolation process of the advected variables are termed solution points, and their placement is determined by a selected quadrature. After this, we calculate the advective fluxes using $u_k$ and $\alpha_k$ interpolated, consequently, also discontinuous. We obtain the continuous fluxes by applying a correction to the discontinuous flux using an approximate Riemann solver [30].

In this work, the quadrature used for the location of solution points was that of the Gauss-Lobatto. For correction functions ($g_R$ and $g_L$), were used the nodal Discontinuous Galerkin polynomials [22], [31], and the Riemann solver used was the Roe solver [30].

After the reconstruction, the advective term of the continuity equations, is expressed as:

$$\frac{\partial(\alpha_k\rho_k)_i^D}{\partial t} = -\frac{2}{(x_{i+1}-x_i)}\sum_{j=1}^{P+1}\left[(\widehat{\alpha_k\rho_k u_k})_{i,j}^D \frac{dL_j}{ds} + \left((\alpha_k\rho_k u_k)_{i-\frac{1}{2}} - (\widehat{\alpha_k\rho_k u_k})_{i,\ i-\frac{1}{2}}^D\right)\frac{dg_L}{ds} + \left((\alpha_k\rho_k u_k)_{i+\frac{1}{2}} - (\widehat{\alpha_k\rho_k u_k})_{i,\ i+\frac{1}{2}}^D\right)\frac{dg_R}{ds}\right] \tag{3}$$

and the momentum equations as:

$$\frac{\partial u_{k_i}^D}{\partial t} = -\frac{2u_k}{(x_{i+1}-x_i)}\sum_{j=1}^{P+1}\left[\widehat{u_k}_{i,j}^D \frac{dL_j}{ds} + \left(u_{k_{i-\frac{1}{2}}} - \widehat{u_k}_{i,\ i-\frac{1}{2}}^D\right)\frac{dg_L}{ds} + \left(u_{k_{i+\frac{1}{2}}} - \widehat{u_k}_{i,\ i+\frac{1}{2}}^D\right)\frac{dg_R}{ds}\right] + \frac{1}{\alpha_k\rho_k}RHS \tag{4}$$

where the superscript $D$ indicates the discontinuous variables and the superscript ^ indicates the parameterized variables to $s$ space, according to $s = \{2[(x - x_i)/(x_{i+1} - x_i)] - 1\}$. The subscribed $i$ is the control volume index and the subscribed $j$ is the solution point index. $P$ is the polynomial degree of solution interpolation, $L$ is the Lagrange polynomial and $RHS$ is the right-hand side of eq. (2).

The velocities and volume fraction fields of two-fluid model are solved using the FR method. In the construction of the mesh for the FR, velocities and volumetric fractions are stored at the solution points in a manner co-localized. The pressure field continues to be balanced at the centers of the CVs. In Fig. 1, the grid is shown with solution points for a case that two points are used for to reconstruct first degree polynomials (FR-P2).

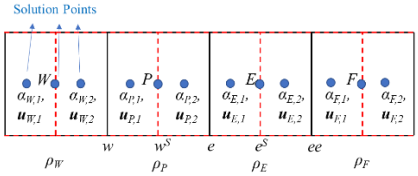



Figure 1. Control volumes with solution points for FR-P2.

The semi-implicit pressure-based method SIMPLE [32] was used to couple the momentum and continuity equations. A pressure-correction equation was used to allow the pressure field to be updated. It was derived from the sum of the mass conservation equations for liquid and gas, dividing each equation by the representative values of the corresponding density [13]. The pressure equation is solved through the Two-Point Flux Approximation (TPFA) finite volume technique using a staggered grid arrangement.

The global algorithm uses a predictor-corrector scheme [29]. The resolution steps follow, inside a loop, the following steps, until a certain tolerance is achieved:

1. Solve momentum equations for velocities, using the pressure field of previous iteration;
2. Solve pressure-correction equation, using the new velocity fields;
3. Update pressure, velocity, and density fields, using the pressure increment;
4. Solve continuity equations for volume fractions;
5. Updates the variables and checks if the tolerance has been reached.

# 4 Results

### 4.1 Transport problem with a non-linear flux and a smooth solution

In this example, we analyze a basic non-linear system that, during the smooth phase of the solution, reduces to the inviscid Burgers' equation [28]. This situation can be regarded as a specific instance of Eq. (2). Within these conditions, the Burgers' equation takes the following conservative form:

$$\frac{\partial u}{\partial t} + \frac{\partial F(u)}{\partial x} = 0 \tag{5}$$

where $F(u) = u^2/2$.

Periodic boundary conditions are applied at the domain boundaries. The initial condition is described as:

$$u(x, t = 0) = \frac{1}{2\pi}\sin(2\pi x), \quad \forall x \in \Omega \tag{6}$$

where $\Omega = [0, 1]$.

The convergence behavior of the FR approach is analyzed using correction functions that correspond to simplified formulations of the NDG and SD methods. For benchmarking, we also include results obtained with the FOU and MUSCL schemes. The evaluation involves computing the $L_1$-norm ($E_{L1}$) of the errors and its associated convergence rate ($R_{L1}$) for the smooth solution at t = 0.5 s [28]. These results are summarized in Table 1. The numerical experiments were performed on a sequence of progressively refined meshes, ranging from 32 to 512 control volumes, following a methodology similar to that of Galindez-Ramirez et al. [24]. For all meshes, we have adopted a CFL = 0.9 for the FR and FOU schemes, and CFL = 0.45 for the MUSCL scheme.

Table 1. Error and convergence rates for the $L_1$-norm of error of the inviscid Burgers' problem.

| CV | 32 | | 64 | | 128 | | 256 | | 512 | |
|---|---|---|---|---|---|---|---|---|---|---|
| Method | $E_{L1}$ | $R_{L1}$ | $E_{L1}$ | $R_{L1}$ | $E_{L1}$ | $R_{L1}$ | $E_{L1}$ | $R_{L1}$ | $E_{L1}$ | $R_{L1}$ |
| FOU | 4.37E-03 | - | 2.37E-03 | 0.88 | 1.24E-03 | 0.93 | 6.37E-04 | 0.96 | 3.22E-04 | 0.98 |
| MUSCL | 1.35E-03 | - | 3.97E-04 | 1.76 | 1.08E-04 | 1.87 | 2.91E-05 | 1.90 | 7.55E-06 | 1.95 |
| FR-NDG-P1 | 8.90E-04 | - | 2.85E-04 | 1.64 | 8.76E-05 | 1.70 | 2.62E-05 | 1.74 | 7.65E-06 | 1.77 |
| FR-SD-P1 | 1.22E-03 | - | 4.02E-04 | 1.61 | 1.25E-04 | 1.69 | 3.75E-05 | 1.73 | 1.10E-05 | 1.77 |
| FR-NDG-P2 | 3.23E-05 | - | 4.34E-06 | 2.90 | 5.77E-07 | 2.91 | 7.56E-08 | 2.93 | 9.74E-09 | 2.96 |
| FR-SD-P2 | 4.83E-05 | - | 6.71E-06 | 2.85 | 9.15E-07 | 2.87 | 1.22E-07 | 2.91 | 1.59E-08 | 2.94 |
| FR-NDG-P3 | 2.56E-06 | - | 2.14E-07 | 3.58 | 1.77E-08 | 3.60 | 1.47E-09 | 3.59 | 1.25E-10 | 3.56 |
| FR-SD-P3 | 3.49E-06 | - | 2.98E-07 | 3.55 | 2.51E-08 | 3.57 | 2.06E-09 | 3.60 | 1.72E-10 | 3.58 |

Across all evaluated methods, the observed convergence trends align well with the expected theoretical asymptotic accuracy, with the exception of the fourth-order flux reconstruction scheme (FR-P3), which begins to exhibit a slight reduction in convergence rate - an effect also reported in [39]. For this particular test case, increasing the approximation order in the FR method yielded substantial improvements in accuracy. Specifically, when refining to the finest grid (512 control volumes), the transition from second- to third-order led to a reduction in error by approximately three orders of magnitude, and the step from third- to fourth-order provided a further two orders of magnitude decrease. Among the FR variants, FR-NDG consistently delivered lower errors than FR-SD across all tested orders. Nonetheless, for second-order accuracy, even the FR-NDG variant produced errors marginally higher than those of the MUSCL method.

We compare, in Fig. 2, errors and computational cost across all tested schemes. The MUSCL scheme proves slightly faster than the FR variants of the same nominal order. For higher polynomial reconstructions (P2 and P3), FR-NDG consistently surpasses FR-SD in accuracy for this nonlinear case. Moreover, the third-order FR methods (NDG and SD) present a more favorable balance between accuracy and efficiency when compared with MUSCL, FOU, and lower-order FR approaches.

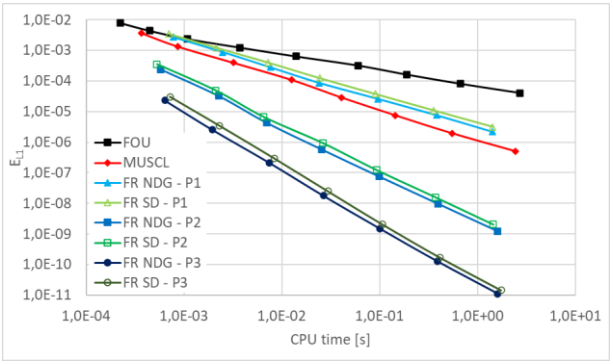



Figure 2. CPU times and norm $L_1$-errors for the 1-D problem with a non-linear flux and a smooth solution.

### 4.2 Water Faucet Problem

The water faucet problem involves a vertical duct, 12 meters in length, with water injected at the top. The injected water accelerates due to gravity, and as a result of the pressure gradient formed, air influx occurs at the bottom of the duct [33]. Initially, the duct is uniformly filled with a void fraction of $\alpha_G$ = 0.2, as shown in Fig. 3. With water injected at 10 m/s, causing a shock in the volumetric fractions.

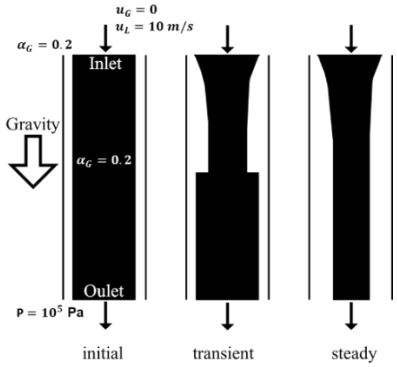



Figure 3. Water faucet problem: Initial configuration (left), transient profile (center) and steady state solution (right).

Just like in the previous case, the solutions are obtained using 32 to 1024 CVs for time t = 0.4 s. In Table 2, we compute the $L_1$-norm of the errors and the convergence rates of the results of the air void fraction ($\alpha_G$). For this case, we used CFL = 0.5 for the FR and FOU schemes, and CFL = 0.25 for the MUSCL scheme.

Given the characteristics of this test case, which involves shock advection, the expected convergence rates are not fully achieved. This behavior is attributed to the use of slope limiters within the numerical schemes—an essential mechanism to preserve stability at the shock interface. As a result, all FR-based approaches produced comparable outcomes, with FR-P2 and FR-P3 configurations, regardless of the correction function employed, yielding the smallest error levels. Another notable observation is that, even at second-order accuracy, the FR method exhibited lower numerical diffusion than the MUSCL scheme.

Table 2. $L_1$-norm of errors for Water Faucet case.

| CV | 32 | | 64 | | 128 | | 256 | | 512 | |
|---|---|---|---|---|---|---|---|---|---|---|
| Method | $E_{L1}$ | $R_{L1}$ | $E_{L1}$ | $R_{L1}$ | $E_{L1}$ | $R_{L1}$ | $E_{L1}$ | $R_{L1}$ | $E_{L1}$ | $R_{L1}$ |
| FOU | 3.73E-01 | - | 2.58E-01 | 0.53 | 1.72E-01 | 0.58 | 1.15E-01 | 0.58 | 7.83E-02 | 0.56 |
| MUSCL | 2.82E-01 | - | 1.82E-01 | 0.63 | 1.13E-01 | 0.70 | 7.17E-02 | 0.65 | 4.94E-02 | 0.54 |
| FR-NDG-P1 | 2.60E-01 | - | 1.62E-01 | 0.69 | 9.80E-02 | 0.72 | 6.36E-02 | 0.63 | 4.59E-02 | 0.47 |
| FR-SD-P1 | 2.63E-01 | - | 1.63E-01 | 0.69 | 9.86E-02 | 0.72 | 6.39E-02 | 0.63 | 4.61E-02 | 0.47 |
| FR-NDG-P2 | 2.51E-01 | - | 1.55E-01 | 0.70 | 9.44E-02 | 0.71 | 6.42E-02 | 0.56 | 4.66E-02 | 0.46 |
| FR-SD-P2 | 2.51E-01 | - | 1.55E-01 | 0.70 | 9.43E-02 | 0.71 | 6.41E-02 | 0.56 | 4.66E-02 | 0.46 |
| FR-NDG-P3 | 2.48E-01 | - | 1.49E-01 | 0.73 | 9.44E-02 | 0.66 | 6.45E-02 | 0.55 | 3.73E-02 | 0.79 |
| FR-SD-P3 | 2.48E-01 | - | 1.49E-01 | 0.73 | 9.44E-02 | 0.66 | 6.45E-02 | 0.55 | 3.73E-02 | 0.79 |

In Fig. 4, we present a zoom of the results of the air void fraction ($\alpha_G$) of a part of the meshes. It is now clear visually that FRs have better accuracy than FOU and MUSCL.

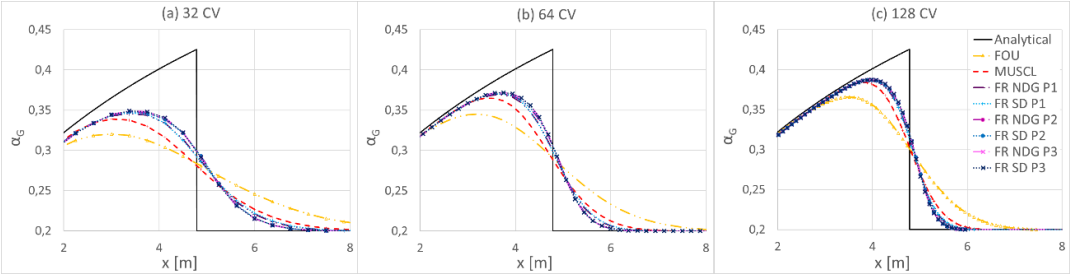



Figure 4. Air void fraction ($\alpha_G$), t = 0.4 s, for different grid resolutions (32, 64 and 128 CVs) and different methods (FOU, MUSCL, FR-NDG-P1, P2, P3 and for FR-SD-P1, P2 and P3).

## 5 Conclusions

In this work, the FR method was implemented in the two-fluid single-pressure model. The method is used to solve the momentum conservation equations and the mass conservation equations. The results demonstrate that the method provides considerable improvements in accuracy. In the first example, FR schemes were successfully tested and showed convergence rates close to nominal. In the Water Faucet Problem, again, it was possible to observe the excellent accuracy of the FR schemes in the adopted model. The in-house implementation proved to be efficient for solving the cases studied. We plan to extend this work to more complex flow scenarios, including thermal effects (two-fluid five-equation model) and others flow patterns.

**Acknowledgements.** The authors would like to thank Petrobras (project number 2023/00049-1), FACEPE (IBPG-0009-3.01/21) and CNPq (process number PQ-308334/2019-1 and PQ-310145/2021-0) for their financial support.

## References

[1] J. Su, “Flow assurance of deepwater oil and gas production - A review”. In: *Proceedings of the International Conference on Offshore Mechanics and Arctic Engineering - OMAE*, 2003. doi: 10.1115/OMAE2003-37144.

[2] “ALFAsim Artificial Lift and Flow Assurance Simulator Technical Manual Written by: ESSS.” [Online]. Available: www.esss.co

[3] T. J. Danielson, K. M. Bansal, B. Djoric, E.-D. Duret, S. T. Johansen and O. Hellan, “Testing and Qualification of a New Multiphase Flow Simulator”. In: *Offshore Technology Conference*, Houston, 2011. doi: 10.4043/21417-ms.

[4] K. H. Bendlksen, D. Malnes, R. Moe and S. Nuland, “Dynamic two-fluid model OLGA. Theory and application”. *SPE Production Engineering*, vol. 6, n. 2, 1991, doi: 10.2118/19451-pa.

[5] M. Jerez-Carrizales, J. E. Jaramillo and D. Fuentes, “Ingeniería y Ciencia Prediction of Multiphase Flow in Pipelines: Literature Review Prediction of Multiphase Flow in Pipelines: Literature Review”. *Ing. Cienc*, vol. 11, n. 22, 2015, doi: https://doi.org/10.17230/ingciencia.11.22.10.

[6] M. Ishii and T. Hibiki. *Thermo-fluid dynamics of two-phase flow*. Springer Nature, 2006. doi: 10.1007/978-0-387-29187-1.

[7] A. Prosperetti and G. Tryggvason. *Computational methods for multiphase flow*. Cambridge University Press, 2007. doi: 10.1017/CBO9780511607486.

[8] I. Toumi, “An upwind numerical method for two-fluid two-phase flow models”. *Nuclear Science and Engineering*, vol. 123, n. 2, 1996, doi: 10.13182/NSE96-A24180.

[9] H. Pokharna, M. Mori and V. H. Ransom, “Regularization of Two-Phase Flow Models: A Comparison of Numerical and Differential Approaches”. *J Comput Phys*, vol. 134, n. 2, 1997, doi: 10.1006/jcph.1997.5695.

[10] M. Pourgol-Mohammad, “Thermal-hydraulics system codes uncertainty assessment: A review of the methodologies”. *Ann Nucl Energy*, vol. 36, n. 11–12, 2009, doi: 10.1016/j.anucene.2009.08.018.

[11] M. L. De Bertodano, W. Fullmer, A. Clausse and V. H. Ransom. *Two-fluid model stability, simulation and chaos*. Springer Nature, 2016. doi: 10.1007/978-3-319-44968-5.

[12] D. Bestion, "The physical closure laws in the CATHARE code". *Nuclear Engineering and Design*, vol. 124, n. 3, 1990, doi: 10.1016/0029-5493(90)90294-8.

[13] Z. Wang, J. Gong and C. Wu, "Numerical simulation of one-dimensional two-phase flow using a pressure-based algorithm". *Numeri Heat Transf A Appl*, vol. 68, n. 4, 2015, doi: 10.1080/10407782.2014.986383.

[14] H. Städtke. *Gasdynamic Aspects of Two-Phase Flow: Hyperbolicity, Wave Propagation Phenomena, and Related Numerical Methods*. Wiley, 2007. doi: 10.1002/9783527610242.

[15] B. van Leer, "Towards the ultimate conservative difference scheme. V. A second-order sequel to Godunov's method". *J Comput Phys*, vol. 32, n. 1, 1979, doi: 10.1016/0021-9991(79)90145-1.

[16] Z. J. Wang, "Spectral (finite) volume method for conservation laws on unstructured grids. Basic Formulation". *J Comput Phys*, vol. 178, n. 1, 2002, doi: 10.1006/jcph.2002.7041.

[17] Z. J. Wang and Y. Liu, "The spectral difference method for the 2D Euler equations on unstructured grids". In: *17th AIAA Computational Fluid Dynamics Conference*, 2005. doi: 10.2514/6.2005-5112.

[18] Z. J. Wang and Y. Liu, "Spectral (Finite) Volume Method for Conservation Laws on Unstructured Grids III: One Dimensional Systems and Partition Optimization". *J Sci Comput*, vol. 20, n. 1, 2004, doi: 10.1023/A:1025896119548.

[19] Z. J. Wang and Y. Liu, "Spectral (finite) volume method for conservation laws on unstructured grids. II. Extension to two-dimensional scalar equation". *J Comput Phys*, vol. 179, n. 2, 2002, doi: 10.1006/jcph.2002.7082.

[20] Z. J. Wang and Y. Liu, "Extension of the spectral volume method to high-order boundary representation". *J Comput Phys*, vol. 211, n. 1, 2006, doi: 10.1016/j.jcp.2005.05.022.

[21] Y. Liu, M. Vinokur and Z. J. Wang, "Discontinuous Spectral Difference Method for Conservation Laws on Unstructured Grids". *Computational Fluid Dynamics*, pp. 449-454, 2004. doi: 10.1007/3-540-31801-1_63.

[22] H. T. Huynh, "A flux reconstruction approach to high-order schemes including discontinuous Galerkin methods". In: *Collection of Technical Papers - 18th AIAA Computational Fluid Dynamics Conference*, 2007. doi: 10.2514/6.2007-4079.

[23] F. R. L. Contreras, D. K. E. Carvalho, G. Galindez-Ramirez and P. R. M. Lyra, "A non-linear finite volume method coupled with a modified higher order MUSCL-type method for the numerical simulation of two-phase flows in non-homogeneous and non-isotropic oil reservoirs". *Computers and Mathematics with Applications*, vol. 92, 2021, doi: 10.1016/j.camwa.2021.03.023.

[24] G. Galindez-Ramirez, D. K. E. Carvalho, and P. R. M. Lyra, "Numerical simulation of 1-D oil and water displacements in petroleum reservoirs using the correction procedure via reconstruction (CPR) method". *Comput Geosci*, vol. 24, n. 1, 2020, doi: 10.1007/s10596-019-09884-x.

[25] G. Galindez-Ramirez, F. R. L. Contreras, D. K. E. Carvalho, and P. R. M. Lyra, "Numerical simulation of two-phase flows in 2-D petroleum reservoirs using a very high-order CPR method coupled to the MPFA-D finite volume scheme". *J Pet Sci Eng*, vol. 192, 2020, doi: 10.1016/j.petrol.2020.107220.

[26] G. Galindez-Ramirez, F. R. L. Contreras, D. K. E. Carvalho and P. R. M. Lyra, "A very high-order flux reconstruction approach coupled to the MPFA-QL finite volume method for the numerical simulation of oil-water flows in 2D petroleum reservoirs". *Appl Math Model*, vol. 106, 2022, doi: 10.1016/j.apm.2022.02.023.

[27] G. Galindez-Ramirez, M. R. A. Souza, D. K. E. Carvalho and P. R. M. Lyra, "Numerical simulation of 1-D oil and water displacements in petroleum reservoirs using the spectral finite volume method". *Journal of the Brazilian Society of Mechanical Sciences and Engineering*, vol. 39, n. 7, 2017, doi: 10.1007/s40430-017-0795-8.

[28] M. E. S. Galindo, I. V. Lacerda, G. Galindez-Ramirez, P. R. M. Lyra and D. K. E. Carvalho, "A very high order Flux Reconstruction (FR) method for the numerical simulation of 1-D compositional fluid flow model in petroleum reservoirs". *Geoenergy Science and Engineering*, vol. 229, 2023, doi: 10.1016/j.geoen.2023.212056.

[29] S. Morales-Ruiz, J. Rigola, I. Rodriguez and A. Oliva, "Numerical resolution of the liquid-vapour two-phase flow by means of the two-fluid model and a pressure based method". *International Journal of Multiphase Flow*, vol. 43, 2012, doi: 10.1016/j.ijmultiphaseflow.2012.03.004.

[30] P. L. Roe. *Characteristic-Based Schemes for the Euler Equations.* Annual Review of Fluid Mechanics, vol. 18. 1986. doi: 10.1146/annurev.fluid.18.1.337.

[31] J. S. Hesthaven and T. Warburton. *Nodal Discontinuous Galerkin Methods: Algorithms, Analysis, and Applications*. Springer, 2007.

[32] S. V. Patankar. *Numerical heat transfer and fluid flow*. CRC Press, 1980, doi: 10.13182/nse81-a20112.

[33] V. H. Ransom, "Numerical Benchmark Test No. 2.1: Faucet Flow". *Multiphase Science and Technology*, vol. 3, n. 1–4, 1987, doi: 10.1615/multscientechn.v3.i1-4.280.